5 Equilibrium Profiles of Glaciers

5.1 PERFECT PLASTICITY

The rate of deformation of glacier ice under its own weight is described by the constitutive relation discussed in Chapter 2. According to the commonly used flow law (2.10), the rate of deformation increases with the third power of the applied stress. In Figure 5.1 this relation is shown schematically. Also shown are two other common forms of rheologic behavior, namely, Newtonian (linear) viscosity and perfect plasticity.

For a Newtonian material, the rate of deformation is linearly dependent on the applied stress, with the constant of proportionality termed the viscosity. In many models for glacier flow, ice is approximated as a Newtonian material to find an analytical solution to the problem under study (see, for example, the model for along-flow variations in ice flow described in Section 4.6). This approximation is valid only where the effective stress is constant over the entire thickness of the glacier. Where this assumption is not valid, effects of the depth-variation in effective stress, and perhaps temperature also, can be included in the linear-viscosity model by prescribing a depth dependency of the viscosity (for example, Whillans and Johnsen, 1983).

A material exhibits perfect plasticity if deformation is negligible when the applied stress is below some critical value, the *yield stress*. For stresses larger than the yield stress, the material deforms "instantly" to relieve the applied stress. As a result, the stress in the material never exceeds the yield stress. Comparison of the curves shown in Figure 5.1 suggests that, at least for larger stresses, glacier flow may be treated as a problem in plasticity (Orowan, 1949; Nye, 1951; Reeh, 1982). In effect, this is equivalent to taking the limit $n \to \infty$ for the exponent in the flow law. Making the perfect plasticity approximation allows the geometry of a glacier to be determined with a minimum of information. While this may not be realistic, it is often the best one can do, especially when reconstructing the large ice sheets that covered the American and European continents during the last glacial period.

Neglecting the effects of gradients in longitudinal stress and lateral drag, the driving stress is balanced by drag at the glacier bed, and the shear stress, τ_{xz}, increases linearly with depth from zero at the surface to the value of the basal drag at the bed (c.f. Section 4.2). Assuming perfect plasticity, the stress in the ice cannot exceed the

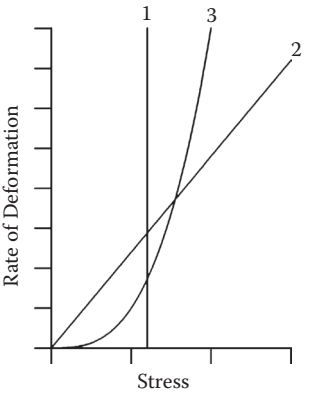

FIGURE 5.1 Rate of deformation as a function of applied stress for three commonly used rheological models. Curve 1 corresponds to a perfectly plastic material, curve 2 represents a linear-viscous material (Newtonian viscosity), and curve 3 corresponds to glacier ice deforming according to Glen's law with exponent n = 3.

yield stress, τ_o, and basal drag must be equal to τ_o. Equating basal drag to the driving stress, it follows immediately that the driving stress is constant, so that

$$-\rho g H \frac{\partial h}{\partial x} = \tau_o, \tag{5.1}$$

where H represents the ice thickness and h the surface elevation. It may be noted that the assumptions made above are perhaps unnecessarily strict. A more general derivation is presented by Nye (1951). His analysis, although more complex because normal stress components are also included, gives essentially the same result for the shear stress, and also leads to equation (5.1) linking the driving stress to the yield stress.

Making the assumption that the glacier rests on a horizontal bed ($\partial h/\partial x = \partial H/\partial x$), equation (5.1) can be integrated to give

$$H^2 = C - \frac{2\tau_o}{\rho g} x. \tag{5.2}$$

The integration constant, C, can be determined from the condition that the ice thickness must be zero at the edge of the glacier. Denoting the half-width of the glacier by L, this constant is found to be

$$C = \frac{2\tau_o}{\rho g} L, \tag{5.3}$$

and

$$H^2 = \frac{2\tau_o}{\rho g}(L - x). \tag{5.4}$$

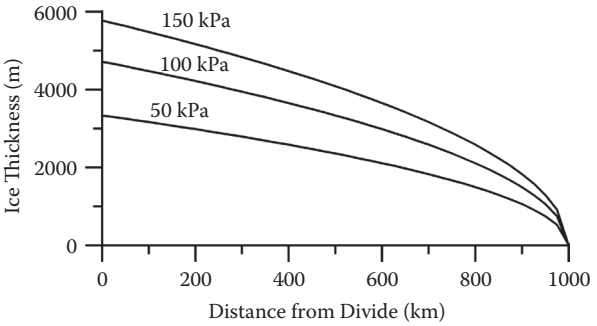

FIGURE 5.2 Flowline profiles of a perfectly plastic ice sheet resting on a flat bed. Labels give the value for the yield stress used in each calculation.

The thickness at the divide (x = 0) is given by

$$H_o = \left(\frac{2\tau_o}{\rho g} L \right)^{1/2}, \tag{5.5}$$

and the profile of the plastic ice sheet can be written as

$$H = H_o \left(1 - \frac{x}{L} \right)^{1/2}. \tag{5.6}$$

The elevation decreases parabolically toward the glacier edge; the surface slope at the margin becomes infinite. Examples calculated for different values of the yield stress are shown in Figure 5.2.

In deriving the parabolic profile, continuity of mass is not considered. Of course, integrated over the entire glacier, snowfall must be larger than ablation to prevent the glacier from wasting away. However, any increase in snowfall has no effect on the ice-sheet profile but is compensated by an increase in ice discharge toward the glacier edge. This admittedly unrealistic behavior is the result of the decoupling between stresses and strain rates in the plastic approach.

For steady-state conditions, the discharge velocity, U, can be derived from conservation of mass. The mass flux through a vertical cross-section of unit width is equal to the discharge velocity (the vertically averaged velocity in the mean direction of flow) times the local ice thickness. To maintain steady state, the mass flux at any location must be equal to the integrated upstream accumulation. That is,

$$HU = \int_0^x M(\bar{x})\, d\bar{x}, \tag{5.7}$$

where M represents the net surface accumulation (snowfall minus melting). Taking M constant along the flowline, it follows that the mass flux must increase linearly

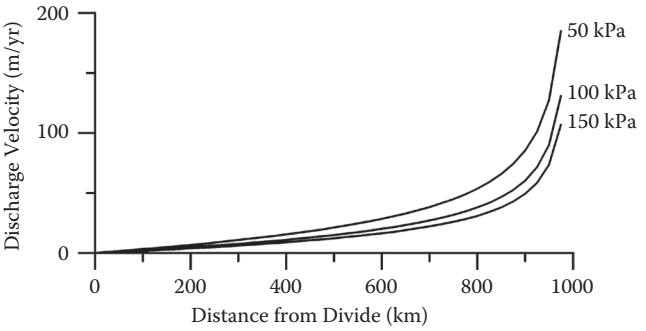

FIGURE 5.3 Discharge velocities required to maintain steady state for the ice-sheet profiles shown in Figure 5.2. The accumulation rate was set to 0.1 m of ice per year.

with distance from the divide. Eliminating the ice thickness using equation (5.6), the discharge velocity is found to be

$$U = \frac{Mx}{H_o}\left(1 - \frac{x}{L}\right)^{1/2}. \tag{5.8}$$

The discharge velocities corresponding to the profiles in Figure 5.2 are shown in Figure 5.3.

At the terminus of the glacier, the model fails. As $x \rightarrow L$, the ice thickness goes to zero and the discharge velocity must go to infinity to maintain the required discharge. This shortcoming is not unique to the plastic model. Most steady-state models in which the ice thickness approaches zero at the glacier terminus predict velocities that become unrealistically large near the snout.

The plasticity approach can be extended to include the second horizontal dimension and to reconstruct the steady-state shape of a three-dimensional ice sheet (Reeh, 1982). On a flat bed, the parabolic profile (5.6) applies to flowlines that are perpendicular to the elevation contours. Because the margin constitutes an elevation contour (namely, $H = 0$), flowlines are perpendicular to the margin and remain straight when traced toward the interior. This means that where the margin is convex, the upstream region of the ice sheet exhibits divergent flow, and ice divides may develop that run inland from the margins. A concave margin, on the other hand, indicates convergent flow upstream, which may feed into ice streams (Reeh, 1982). Where the bed is not horizontal, deflection of flowlines may occur; an analytical expression for the profile cannot be readily derived, and numerical methods have to be used.

Perhaps the most valuable application of the perfect-plasticity approximation is the reconstruction of former ice sheets. Out of necessity, such reconstructions are often based on sparse geological observations of glacial landforms such as end moraines that indicate the maximum extent of the former glacier and other geological markings that indicate the nature of the former flow regime as well. For example, striated pavements suggest that basal sliding was important, while till sheets may be indicative of streaming flow. Combining various sources of information, Denton and

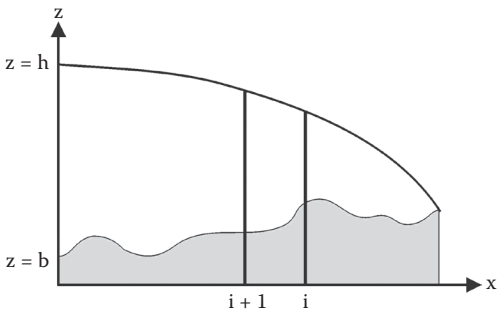

FIGURE 5.4 Geometry used in the numerical solution scheme for reconstructing the profile of a glacier on an arbitrary bed topography, using the perfectly plastic approximation. Note that the gridpoint number, i, increases toward the interior.

Hughes (1981) and Hughes (1985) present possible reconstructions of the Cenozoic ice sheet during the time of maximum extent.

The reconstruction scheme is based on equation (5.1), which is solved numerically on discrete gridpoints, starting at the glacier margin and proceeding upglacier. To do so, the continuous derivative of the surface elevation is discretized as (see Figure 5.4 for the notation used)

$$\frac{\partial h}{\partial x} = \frac{h_i - h_{i+1}}{\Delta x}, \tag{5.9}$$

noting that the x-axis is directed from the ice-sheet center toward the margin. The subscript i refers to gridpoints, with i = 1 denoting the position of the ice margin (where calculations start), while Δx is the horizontal spacing between adjacent gridpoints. Equation (5.1) can thus be rewritten to give (Schilling and Hollin, 1981; Hughes, 1985)

$$h_{i+1} = h_i + \left(\frac{\tau_o}{H}\right)\frac{\Delta x}{\rho g}. \tag{5.10}$$

To be fully correct, the yield stress and ice thickness, appearing on the right-hand side of this expression, should be evaluated at i + 1/2. Multiplying equation (5.10) by the ice thickness gives

$$(h_{i+1} - h_i)H_{i+1/2} - \frac{2\,\Delta x\,\overline{\tau}_o}{\rho g} = 0. \tag{5.11}$$

Denoting the bed elevation by b_i (positive when above sea level), the ice thickness is $H_i = h_i - b_i$. Evaluating the thickness over the grid interval from the average of the two values at the surrounding gridpoints, the following equation is found:

$$h_{i+1}^2 - h_{i+1}(b_i + b_{i+1}) + h_i(b_{i+1} - H_i) - \frac{2\Delta x\,\overline{\tau}_o}{\rho g} = 0, \tag{5.12}$$

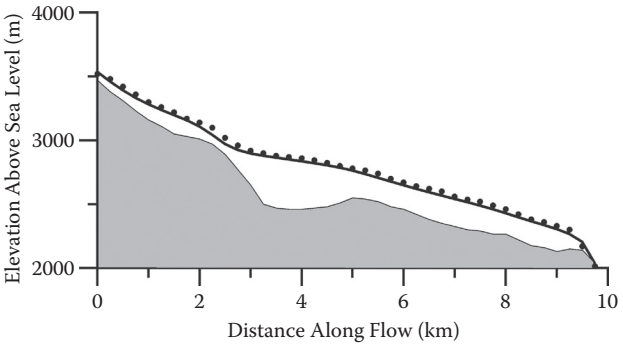

FIGURE 5.5 Reconstructed and measured profile of the Rhône Glacier, France. Measured surface (dots) and basal topography are from Stroeven, A., R. van de Wal, and J. Oerlemans (1989). The reconstructed profile was calculated using the perfectly plastic approximation with a yield stress of 200 kPa.

where the overbar indicates that the average value of the yield stress over the grid interval is to be used.

The advantage of using equation (5.12) instead of the more simple version (5.10) is that the first equation can also be applied at the margin to calculate the surface elevation at the next upglacial gridpoint (i.e., h_2). This is not the case when equation (5.10) is used, because the ice thickness is zero at the margin. Instead, h_2 must be estimated from, for example, the parabolic solution (equations (5.5) and (5.6)) if the bed near the margin is flat, or from the solutions that apply to a sloping bed derived in Nye (1952b) (c.f. Schilling and Hollin, 1981).

A comparison between a "reconstructed" and an actual glacier profile is shown in Figure 5.5. The glacier considered is the Rhône Glacier in the French Alps, for which the surface and bed elevations are tabulated in Stroeven et al. (1989). The reconstructed surface profile was obtained using a yield stress of 200 kPa. This may seem like a large value for a relatively small valley glacier. However, the width of the glacier is about 1 to 2 km (Stroeven et al., 1989), and lateral drag may be expected to be important. Because the driving stress is equated to the yield stress, τ_o, basal drag is $f\tau_o$, where f represents the shape factor (c.f. Section 4.3). An appropriate value for the shape factor is 0.7 to 0.8, giving a basal drag of 140 to 160 kPa.

In the examples discussed so far, the yield stress is taken constant for the entire glacier. However, where basal sliding occurs, the drag at the glacier bed may be expected to be smaller than would be the case for a frozen bed. To include this in the perfectly plastic model, a smaller yield stress can be prescribed in areas where sliding is believed to have occurred (as inferred, for example, from glacial striae). The effect of lowering the yield stress is to lower the surface slope. To illustrate this, Figure 5.6 shows two reconstructed profiles, one calculated with a yield stress decreasing toward the ice-sheet edge, and one with a constant yield stress (chosen such that for both ice sheets, the average yield stress is the same).

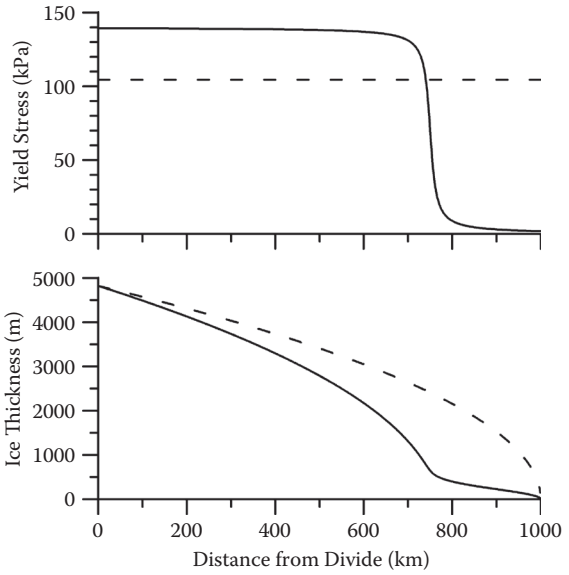

FIGURE 5.6 Comparison of ice-sheet profiles calculated using a constant yield stress (dashed curve) and using a yield stress decreasing near the margin. The average yield stress is the same for both glaciers.

As noted earlier, the models discussed above do not invoke mass continuity. One way to satisfy conservation of mass is to use either the lamellar flow theory or a sliding relation to link the ice velocity to basal drag and hence to the yield stress. The ice velocity is calculated from the continuity equation for mass. Thus, an expression for the yield stress along the glacier can be derived and substituted into equation (5.12) to allow the glacier profile to be calculated (for example, Hughes, 1985). Although the solution scheme becomes more complicated, the essential idea is similar to the models described above.

5.2 CONTINUITY EQUATION

An important requirement for (numerical) models of glaciers is that no ice may be created or lost: thickness changes at any particular point must be entirely due to the ice flow and local snowfall or melting. Integrated over the entire glacier, the average rate of thickness change must equal the total amount of ice added at the surface through snowfall minus losses from melting and calving at the glacier terminus. This conservation of mass is expressed by the continuity equation. Because the density of ice is usually taken constant (thus neglecting densification in the upper firn layers), mass conservation corresponds to conservation of ice volume.

To derive the continuity equation for an ice column extending from the bed to the surface, consider Figure 5.7. For clarity, flow in one direction only (along the x-axis) is considered; extension to include the second horizontal direction is straightforward.

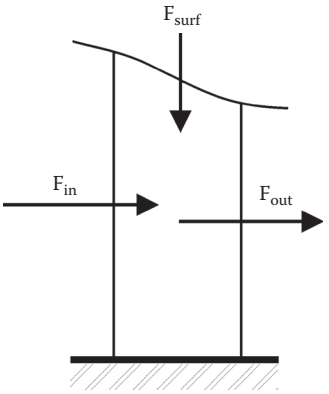

FIGURE 5.7 Mass fluxes in and out of a vertical column extending from the bed to the surface.

By definition, the ice flux through any vertical section is equal to HU, being the amount of ice flowing through the section per unit time and unit width in the cross-flow direction. The ice flux into the column of unit width is thus

$$F_{in} = HU(x), \tag{5.13}$$

and the flux out of the column is

$$F_{out} = HU(x+\Delta x). \tag{5.14}$$

The accumulation rate, M, is the amount of snowfall or ablation expressed in meters of ice depth per unit time and unit area (if basal melting occurs, this can also be included in M; usually the rate of basal melting is negligible compared to the surface accumulation or ablation). Hence, the ice input at the surface is (per unit width):

$$F_{surf} = M\Delta x. \tag{5.15}$$

When these three fluxes are not in balance, the column must become either thicker or thinner. The rate of thickness change is $\partial H/\partial t$, and the corresponding change in volume of the column is (per unit time and unit width)

$$\frac{\partial H}{\partial t}\Delta x. \tag{5.16}$$

Conservation of mass (or volume) is now expressed by

$$\frac{\partial H}{\partial t}\Delta x = F_{in} - F_{out} + F_{surf} = \\ = HU(x) - HU(x+\Delta x) + M\Delta x. \tag{5.17}$$

Dividing both sides by Δx and taking the limit $\Delta x \to 0$ gives the continuity equation

$$\frac{\partial H}{\partial t} = -\frac{\partial (H U)}{\partial x} + M. \tag{5.18}$$

This equation states that the thickness may change as a result of flow divergence (first term on the right-hand side) and due to local accumulation or ablation (second term on the right-hand side). To account for flow in the second horizontal direction, a term describing divergence of flow in that direction can be added to the right-hand side.

A more formal derivation of the continuity equation is based on the incompressibility condition (1.39)

$$\frac{\partial u}{\partial x} + \frac{\partial v}{\partial y} + \frac{\partial w}{\partial z} = 0, \tag{5.19}$$

where u, v, and w represent the three components of velocity in the three orthogonal directions x, y, and z. The z-axis is chosen vertical and positive upward, while x and y represent the two horizontal directions. Because the density of ice is assumed constant, this equation can be considered the local continuity equation (c.f. Lliboutry, 1987c, p. 50).

Integrating equation (5.19) with respect to z from the base (z = b) to the surface (z = h) gives

$$w(h) - w(b) = -\int_b^h \frac{\partial u}{\partial x}\, dz - \int_b^h \frac{\partial v}{\partial y}\, dz. \tag{5.20}$$

Using Leibnitz's rule, the order of integration and differentiation can be changed, and

$$\begin{aligned} w(h) - w(b) = &-\frac{\partial}{\partial x}\left(\int_b^h u\, dz\right) + u(h)\frac{\partial h}{\partial x} - u(b)\frac{\partial b}{\partial x} + \\ &-\frac{\partial}{\partial y}\left(\int_b^h v\, dz\right) + v(h)\frac{\partial h}{\partial y} - v(b)\frac{\partial b}{\partial y}. \end{aligned} \tag{5.21}$$

The vertical velocity at the surface is, by definition, the rate of change in surface elevation that is not due to local accumulation (that is, if the glacier is locally thickening because snow is added at the surface, the vertical velocity is zero). Thus

$$\begin{aligned} w(h) \equiv \frac{dh}{dt} - M = \\ = \frac{\partial h}{\partial t} + u(h)\frac{\partial h}{\partial x} + v(h)\frac{\partial h}{\partial y} - M. \end{aligned} \tag{5.22}$$

Similarly, the vertical velocity at the glacier base is

$$w(b) \equiv \frac{db}{dt} + M_b = \\ = \frac{\partial b}{\partial t} + u(b)\frac{\partial b}{\partial x} + v(b)\frac{\partial b}{\partial y} + M_b. \quad (5.23)$$

Here, M_b represents the basal melting rate, taken positive when melting occurs (note that basal melting causes the lower ice surface to move upward).

Substituting expressions (5.22) and (5.23) for the vertical velocity at the surface and base, into the depth-integrated continuity equation (5.21) gives

$$\frac{\partial h}{\partial t} - M - \frac{\partial b}{\partial t} + M_b = -\frac{\partial (HU)}{\partial x} - \frac{\partial (HV)}{\partial y}, \quad (5.24)$$

with the depth-averaged components of velocity, U and V, defined as

$$U = \frac{1}{H}\int_b^h u\,dz, \quad (5.25)$$

and

$$V = \frac{1}{H}\int_b^h v\,dz. \quad (5.26)$$

The ice thickness is given by $H = h - b$, so that equation (5.24) can be rewritten in its familiar form

$$\frac{\partial H}{\partial t} = -\frac{\partial (HU)}{\partial x} - \frac{\partial (HV)}{\partial y} + M - M_b. \quad (5.27)$$

The vertically integrated continuity equation (5.27) expresses conservation of mass for an ice column extending over the entire ice thickness. The left-hand side is the time derivative of the local thickness, making the continuity equation a prognostic equation that can be used to determine ice thickness at a later time when the terms on the right-hand side are known. Divergence of ice flux and surface mass balance can be estimated from diagnostic equations that do not contain a time derivative and that specify a balance of quantities (for example, forces) at any moment in time. In the case of numerical ice-flow models, velocities and surface mass balance are calculated from the current geometry, and the continuity equation then allows the change in glacier geometry to be estimated. Therefore, equation (5.27) is the central equation that is solved in time-marching numerical models (c.f. Chapter 9).

Where surface velocities and ice thickness has been measured, equation (5.24) can be used to estimate the local rate of thickness change. This procedure was applied by Reeh and Gundestrup (1985) to flow along a strain grid to estimate the mass balance of the Greenland Ice Sheet at Dye-3. Taking the x-axis in the direction of flow, the continuity equation becomes

$$\frac{\partial H}{\partial t} = M - \frac{1}{f}\left[H\left(\frac{\partial U_o}{\partial x} + \frac{\partial V_o}{\partial y}\right) + U_o \frac{\partial H}{\partial x}\right], \tag{5.28}$$

where the subscript o indicates measured surface velocities and f is a correction factor accounting for the depth variation in horizontal ice velocity. Perhaps the greatest uncertainty in this calculation derives from the unknown shape of the velocity profiles. Reeh and Gundestrup (1985) argue that f ranges between 1.13 and 1.10. For isothermal lamellar flow, $f = (n + 2)/(n + 1) = 1.25$ for $n = 3$.

5.3 STEADY-STATE PROFILES ALONG A FLOWLINE

Using the continuity equation derived in the previous section, the steady-state profile of an ice sheet can be determined if the discharge velocity can be calculated from the geometry. An analytical solution for the ice thickness along a flowline can be found for only a few very simple cases, including an ice sheet on a flat bed and constant surface accumulation (Vialov, 1958), or for an ice sheet on a flat bed with uniform accumulation in the interior region and uniform ablation in the marginal region (Weertman, 1961c; Paterson, 1972). For more realistic basal topography and surface accumulation or ablation, the continuity equation needs to be integrated numerically to find the steady-state profile.

For lamellar flow, the depth-averaged discharge velocity is given by equation (4.31), with basal sliding set to zero

$$U = -\frac{2AH}{n+2}(\rho g H)^n \left|\frac{\partial h}{\partial x}\right|^{n-1} \frac{\partial h}{\partial x}. \tag{5.29}$$

On a flat bed, $\partial h/\partial x = \partial H/\partial x$, and

$$U = -A_o H^{n+1} \left|\frac{\partial H}{\partial x}\right|^{n-1} \frac{\partial H}{\partial x}, \tag{5.30}$$

with A_0 containing all constants

$$A_o = \frac{2A}{n+2}(\rho g)^n. \tag{5.31}$$

Using equation (5.30) to eliminate the velocity from the continuity equation yields one equation with one unknown (the ice thickness) that can be solved.

For steady state and flow in the x-direction only, the continuity equation (5.27) reduces to

$$\frac{\partial (HU)}{\partial x} = M. \tag{5.32}$$

For surface accumulation, M, constant along the flowline, this may be integrated to give

$$HU = Mx, \tag{5.33}$$

where the boundary condition of no ice flow across the divide (at $x = 0$) has been invoked.

Substituting expression (5.30) for the vertical mean ice velocity into the integrated continuity equation (5.33) gives

$$-A_o H^{n+2} \left|\frac{\partial H}{\partial x}\right|^{n-1} \frac{\partial H}{\partial x} = Mx. \tag{5.34}$$

Rearranging

$$\left(H^{1+2/n} \frac{\partial H}{\partial x}\right)^n = -\frac{M}{A_o} x, \tag{5.35}$$

or

$$\frac{\partial}{\partial x}(H^{2+2/n}) = -\frac{2n+2}{n}\left(\frac{M}{A_o}\right)^{1/n} x^{1/n}. \tag{5.36}$$

Integrating this expression, and using the boundary condition that the thickness is zero at the ice-sheet margin (at $x = L$), the profile is found to be

$$H^{2+2/n} = H_o^{2+2/n}\left[1 - \left(\frac{x}{L}\right)^{1+1/n}\right], \tag{5.37}$$

with

$$H_o^{2+2/n} = \frac{2n+2}{n+1}\left(\frac{M}{A_o}\right)^{1/n} L^{1+1/n}, \tag{5.38}$$

the ice thickness at the divide.

The steady-state solution (5.37) is usually written as

$$\left(\frac{H}{H_o}\right)^{2+2/n} + \left(\frac{x}{L}\right)^{1+1/n} = 1. \tag{5.39}$$

This profile was first derived by Vialov (1958) and is commonly referred to as the Vialov profile. It applies to a glacier that flows by internal deformation only, over a flat bed and with constant rate of surface accumulation.

The steady-state profile of a glacier that is sliding over a (horizontal) bed can be found if Weertman-type sliding is adopted. Basal sliding is discussed in Chapter 7, but for now it suffices to know that this relation links the sliding speed to basal drag raised to the power m. Equating basal drag with driving stress, and assuming a horizontal bed, gives

$$U = - A_{sl} H^m \left| \frac{\partial H}{\partial x} \right|^{m-1} \frac{\partial H}{\partial x}, \tag{5.40}$$

in which A_{sl} is a sliding parameter that depends on the bed roughness; the sliding exponent m equals (1 + n)/2. Note that, apart from the different prefactors, the only difference between this sliding relation and the velocity from internal deformation is a factor H.

Again, the steady-state profile is found by substituting expression (5.40) for the sliding velocity into the continuity equation (5.32) and integrating twice along the flowline. The result is

$$\left(\frac{H}{H_o} \right)^{2+1/m} + \left(\frac{x}{L} \right)^{1+1/m} = 1, \tag{5.41}$$

with

$$H_o^{2+1/m} = \frac{2m + 2}{m + 1} \left(\frac{M}{A_{sl}} \right)^{1/m} L^{1+1/m}. \tag{5.42}$$

Note that in the limit $n \to \infty$, both the profile (5.41) and the profile given by (5.39) reduce to the parabolic profile derived under the perfectly plastic approximation.

The thickness at the ice divide can be calculated from equation (5.38) for the Vialov profile, and from (5.42) for the Weertman-sliding profile. For both profiles, this thickness depends only weakly on the mass balance, M. A doubling of the surface accumulation leads to an increase in H_o of only 9% for the Vialov profile and about 15% for the Weertman-sliding profile (if the length of the ice sheet is kept fixed, and using n = 3 or m = 2). Apparently, the increased accumulation is compensated for by increased discharge, without affecting the geometry of the glacier very much, and the steady-state geometry is rather insensitive to changes in M. In the perfectly plastic approach, the profile is completely independent from M.

A generalization to equilibrium profiles for nonuniform surface mass balance is given by Bueler and others (2005), based on parameterization of the mass flux. On a horizontal bed the mass flux, Q, is given by the left-hand side of equation (5.34). Considering the region $0 \le x \le L$ extending from the ice divide to the margin, the

thickness gradient is negative and the mass flux positive, and this expression can be rewritten as

$$H^{n+2}\left(\frac{\partial H}{\partial x}\right)^n = -\frac{Q}{A_o}. \tag{5.43}$$

Raising both sides to the power 1/n gives

$$H^{(n+2)/n}\frac{\partial H}{\partial x} = -\left(\frac{Q}{A_o}\right)^{1/n}, \tag{5.44}$$

or

$$\frac{n}{2n+2}\frac{\partial}{\partial x}[H^{(2n+2)/n}] = -\left(\frac{Q}{A_o}\right)^{1/n}. \tag{5.45}$$

Integrating from the ice divide (x = 0) to some point x downglacier gives the ice thickness

$$H(x)^{(2n+2)/n} = H_o^{(2n+2)/n} - \frac{2n+2}{n}\frac{1}{A_o^{1/n}}\int_0^x Q(\bar{x})^{1/n}\, d\bar{x}. \tag{5.46}$$

Many functional relations can be adopted for the flux, including the one corresponding to a constant mass balance (which would give the Vialov profile (5.37)). Bueler and others (2005) adopt the following function:

$$Q(x) = C\left[\left(\frac{x}{L}\right)^{1/n} + \left(1-\frac{x}{L}\right)^{1/n} - 1\right]^n, \tag{5.47}$$

where C is a constant to be determined from the boundary condition that the thickness at the margin is zero. The integral of the ice flux is then

$$\int_0^x Q(\bar{x})^{1/n}\, d\bar{x} = C^{1/n} L \frac{n}{n+1}\left[\left(\frac{x}{L}\right)^{(n+1)/n} - \left(1-\frac{x}{L}\right)^{(n+1)/n} + 1 - \frac{n+1}{n}\frac{x}{L}\right]. \tag{5.48}$$

Substituting in equation (5.46) and invoking H(L) = 0 gives

$$C = H_o^{2n+2}\, A_o\left[2L\left(1-\frac{1}{n}\right)\right]^{-n}, \tag{5.49}$$

and the steady-state profile is given by

$$H(x) = \frac{H_o}{(n-1)^{n/(2n+2)}}\left[(n+1)\frac{x}{L} - 1 + n\left(1-\frac{x}{L}\right)^{1+1/n} - n\left(\frac{x}{L}\right)^{1+1/n}\right]^{n/(2n+2)}. \tag{5.50}$$

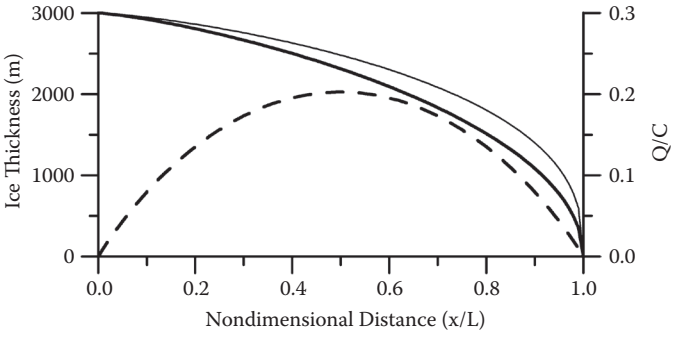

FIGURE 5.8 Steady-state profiles on a horizontal bed, corresponding to the Vialov solution (5.37) for constant mass balance (light curve; equation (5.37)), and to the Bueler profile (5.50); the dashed line (scale on the right) shows the normalized ice flux corresponding to the Bueler profile.

The mass balance corresponding to this steady-state profile is found by differentiating the flux, Q:

$$M(x) = \frac{C}{L}\left[\left(\frac{x}{L}\right)^{1/n} + \left(1-\frac{x}{L}\right)^{1/n} - 1\right]^{n-1}\left[\left(\frac{x}{L}\right)^{(1-n)/n} - \left(1-\frac{x}{L}\right)^{(1-n)/n}\right]. \quad (5.51)$$

A comparison between the Vialov profile (5.37) and the Bueler profile (5.50) is shown in Figure 5.8; the Weertman profile (5.41) is almost indistinguishable from the Vialov profile and not shown in this figure. The dashed line in this figure represents the normalized ice flux, Q/C, adopted by Bueler and others (2005) and reaches a maximum at L/2. Because the surface mass balance equals the divergence of the ice flux, this means that M is negative (ablation) over the lower half of the model ice sheet. For the Vialov profile, M is constant and the ice flux increases linearly from zero at the divide to the value ML at the ice edge. A consequence of this difference between the two profiles is that for the Vialov profile the ice velocity must go to infinity at the margin, whereas in the Bueler model, the velocity at the margin is bounded. Or, equivalently, for the Bueler solution the driving stress at the margin remains finite but is unbounded in the Vialov solution (Greve and Blatter, 2009, p. 89).

5.4 STEADY-STATE PROFILE OF AN AXISYMMETRIC ICE SHEET

In most ice-sheet models discussed in this book, an orthogonal Cartesian coordinate system is used with the three axes perpendicular; the z-axis is chosen vertical (positive upward), while the x-axis and y-axis lie in the horizontal plane. Their orientations may be chosen arbitrarily (but perpendicular to each other), although it is customary to chose the x-axis along the mean direction of flow. In some instances, however, it is more convenient to use a different coordinate system. One example is the axisymmetric ice sheet: such an ice sheet can be rotated around the vertical z-axis without altering the geometry or flow in a fixed location. Another example

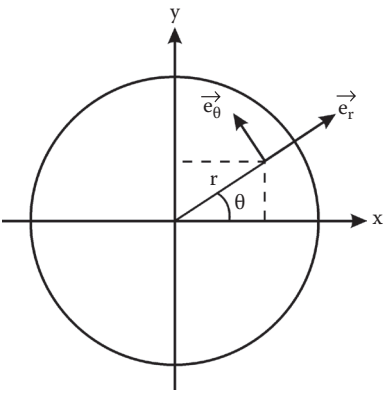

FIGURE 5.9 Relation between Cartesian coordinates, x and y, and radial coordinates, r and θ.

is the modeling of the Northern Hemisphere glacial ice sheets. Rather than using a Cartesian coordinate system, a system based on geographical coordinates (latitude and longitude) is sometimes used (for example, Birchfield et al., 1981; Peltier and Hyde, 1987). A third example, creep closure of englacial tunnels, is discussed in Section 3.6.

The coordinate system used to model an axisymmetric ice sheet is the cylindrical system, in which the coordinates of a point are given by the radius, r, the azimuth angle, θ, and elevation, z (see also Section 3.6). The relation between these coordinates and the Cartesian coordinates follows directly from geometrical considerations (Figure 5.9), and is

$$\begin{aligned} r &= \sqrt{x^2 + y^2}, \\ \tan\theta &= \frac{y}{x}, \end{aligned} \tag{5.52}$$

while the vertical z-coordinate is the same in both systems. To find the model equations in the new coordinate system, one could use the expressions (5.52) to write x and y in terms of r and θ and substitute the result in the Cartesian form of the equations. A simpler and faster way is to write the equations first in a form that is independent of the coordinate system used, and next to use standard mathematical formulas to arrive at the form appropriate for the new coordinate system.

Consider first the depth-integrated ice velocity. For deformational flow the x-component of velocity is proportional to the slope of the surface elevation in the x-direction. Similarly, the y-component of velocity is proportional to the surface slope in the y-direction. Then

$$U = -f(H)\left|\frac{\partial h}{\partial x}\right|^{n-1}\frac{\partial h}{\partial x}, \tag{5.53}$$

and

$$V = -f(H)\left|\frac{\partial h}{\partial y}\right|^{n-1}\frac{\partial h}{\partial y}, \tag{5.54}$$

with

$$f(H) = \frac{2AH}{n+2}(\rho g H)^n. \tag{5.55}$$

These two equations can be combined into one vector equation

$$\vec{U} = -f(H)|\nabla h|^{n-1}\nabla h. \tag{5.56}$$

Here, $\vec{U} = (U,V)$ represents the horizontal velocity vector with components U and V in the (x, y) coordinate system. The symbol ∇ is called the nabla operator (Section 1.1). When applied to a scalar quantity such as the surface elevation, ∇h represents the gradient of h, or the surface slope vector with components $\partial h/\partial x$ and $\partial h/\partial y$ in the (x, y) coordinate system (actually, ∇h is a three-dimensional vector; however, the surface elevation is independent of the vertical z-direction, and the z-component of the vector ∇h is zero and omitted here). Because equation (5.56) is written in vector form, it is independent of the coordinate system used, provided, of course, that the velocity and gradient vectors are referenced to the same coordinate system.

Most mathematics textbooks provide expressions for ∇h applicable to the three most-often used coordinate systems (the Cartesian system, cylindrical coordinates, and polar coordinates). For the cylindrical (r, θ) system, the gradient of the surface is given by (omitting the z-component)

$$\nabla h = \frac{\partial h}{\partial r}\vec{e}_r + \frac{1}{r}\frac{\partial h}{\partial \theta}\vec{e}_\theta, \tag{5.57}$$

where $\vec{e}_r$ and $\vec{e}_\theta$ represent the unit vectors in the r- and θ-directions, respectively (c.f. Figure 5.9). Using this expression in equation (5.56), the two components of ice velocity in the r- and θ-directions can be determined.

The second equation to be considered is the continuity equation (5.27). The first two terms on the right-hand side represent the divergence of ice flux. This is a scalar function, derived from the vector representing the ice flux. In mathematical notation, $\mathrm{div}(H\vec{U}) = \nabla\bullet(H\vec{U})$. Although the nabla symbol is used again, it here represents a vector operator that, when applied to a vector, gives a scalar quantity (the dot signifies the distinction with the earlier use). The continuity equation can now be rewritten as

$$\frac{\partial H}{\partial t} = -\nabla\bullet(H\vec{U}) + M. \tag{5.58}$$

Again, this form of the continuity equation is independent of the coordinate system, provided the nabla operator is referenced to the same coordinate system as the flux vector. In cylindrical coordinates, the divergence of flux becomes

$$\nabla \bullet (H\vec{U}) = \frac{1}{r}\frac{\partial}{\partial r}(r H U_r) + \frac{1}{r}\frac{\partial U_\theta}{\partial \theta}. \tag{5.59}$$

The two components of velocity, U_r and U_θ, can be found by substituting equation (5.57) for the gradient of the surface slope into equation (5.56) for the velocity vector. The radial component of velocity, U_r, is in the direction of $\vec{e}_r$, while the tangential component of velocity, U_θ, is in the direction of $\vec{e}_\theta$.

For an axisymmetric ice sheet, the equations can be simplified because derivatives with respect to θ are zero. Thus, the velocity component in the θ-direction, U_θ, is zero; that is, the ice flows radially outward from the ice divide with a velocity given by (assuming a flat bed so that the surface elevation may be replaced with the ice thickness):

$$U_r = -A_o H^{n+1}\left|\frac{\partial H}{\partial r}\right|^{n-1}\frac{\partial H}{\partial r}. \tag{5.60}$$

For steady state, the continuity equation (5.58) now becomes

$$-\frac{1}{r}\frac{\partial}{\partial r}\left(r A_o H^{n+2}\left|\frac{\partial H}{\partial r}\right|^{n-1}\frac{\partial H}{\partial r}\right) = M. \tag{5.61}$$

As in the previous section, this equation can be integrated twice with respect to r, to yield the thickness profile

$$\left(\frac{H}{H_o}\right)^{2+2/n} + \left(\frac{r}{R}\right)^{1+1/n} = 1, \tag{5.62}$$

where r = R represents the (circular) edge of the ice sheet with H(R) = 0. The ice thickness at the divide is given by

$$H_o^{2+2/n} = \frac{2n+2}{n+1}\left(\frac{M}{2A_o}\right)^{1/n} R^{1+1/n}. \tag{5.63}$$

Comparing the axisymmetric solution (5.62) with the flowline solution (5.39) shows that both profiles are similar (Figure 5.10). The only difference is the thickness at the ice divide. For the same accumulation rate, M, flow parameter, A_o, and horizontal extent (R = L), the axisymmetric ice sheet is thinner by a factor of $(1/2)^{1/n} = 0.79$ (for n = 3). This difference is due to the fact that the flowline model does not account for divergence of flow (that is, the flowband is of constant width and, locally, there is no ice lost due to flow in the transverse direction). The axisymmetric solution includes flow divergence associated with the radially outward flow.

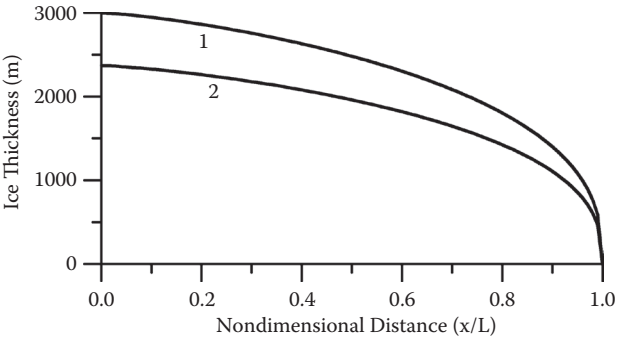

FIGURE 5.10 Steady-state profiles on a horizontal bed, corresponding to the lamellar-flow solution for an ice sheet of constant width (curve 1; equation (5.37)), and for an axisymmetric ice sheet (curve 2; equation (5.62)). For profile 1 the thickness at the center was set to 3000 m; for profile 2 this thickness was reduced by a factor of 0.79. The solution (5.42) for Weertman-type sliding is indistinguishable from curve 1.

5.5 STEADY-STATE PROFILE OF A FREE-FLOATING ICE SHELF

Sanderson (1979) describes how the steady-state profile of an ice shelf can be calculated by numerical integration of the continuity equation. As shown by Van der Veen (1983), an analytical expression for the ice-shelf profile can be derived for the simple case of a free-floating ice shelf spreading in one direction only. The assumption of plane flow implies that the ice thickness, velocity, and strain rate vary only in the direction of flow, and resistance to flow from lateral drag is neglected. Furthermore, vertical shear is neglected (Sanderson and Doake, 1979), and the ice velocity is taken constant with depth.

Under these simplifying assumptions, the along-flow rate of stretching is a function of the ice thickness only, as given by equation (4.64)

$$\dot{\varepsilon}_{xx} = CH^n, \tag{5.64}$$

with the constant, C, defined as

$$C = \left(\frac{\rho g(\rho_w - \rho)}{4B\rho_w} \right)^n, \tag{5.65}$$

in which ρ and ρ_w represent the density of ice and sea water, respectively, and B denotes the viscosity parameter in Glen's flow law (2.12).

The next step is to consider the continuity equation (5.32). Using the definition for the stretching rate as the along-flow gradient in the along-flow component of velocity, U,

$$\dot{\varepsilon}_{xx} = \frac{\partial U}{\partial x}, \tag{5.66}$$

the continuity equation for steady state (i.e., $\partial H/\partial t = 0$) can also be written as

$$H\dot{\varepsilon}_{xx} + U\frac{\partial H}{\partial x} = M. \tag{5.67}$$

For constant accumulation rate, M, the ice flux increases linearly with distance along the flowline (equation (5.33)) and

$$HU = Mx + H_o U_o, \tag{5.68}$$

in which $H_o U_o$ represents the ice flux across the grounding line (at $x = 0$) into the ice shelf. Using this expression to eliminate the velocity from equation (5.67) and substituting (5.64) for the stretching rate gives the following equation:

$$(Mx + H_o U_o)\frac{\partial H}{\partial x} = MH - CH^{n+2}. \tag{5.69}$$

The only unknown in this equation is the ice thickness, H. To solve this equation analytically, three different cases must be considered, namely, $M = 0$ (surface accumulation equals basal melting), $M > 0$ (surface accumulation is larger than basal melting), and $M < 0$ (basal melting exceeds surface accumulation).

If the rate of basal melting equals the rate of surface accumulation, $M = 0$, and the continuity equation (5.69) reduces to

$$\frac{\partial H}{\partial x} = -\frac{C}{H_o U_o}H^{n+2}. \tag{5.70}$$

Integration yields

$$H = \left(\frac{(n+1)C}{H_o U_o}x + H_o^{-(n+1)}\right)^{-1/(n+1)}, \tag{5.71}$$

where the boundary condition $H = H_o$ at the grounding line ($x = 0$) has been used. For $n = 3$, the thickness is proportional to $x^{-1/4}$, and the strongest decrease in ice thickness is found in the vicinity of the grounding line. Farther away from the grounding line, the thickness gradient becomes very small and the thickness tends to reach a constant value (as illustrated by profile a shown in Figure 5.11). Equation (5.70) restricts neither the ice thickness nor the length of the ice shelf, and some criterion must be used to prevent the shelf from becoming infinitely long. In calculating the profile shown in Figure 5.11, the maximum length of the ice shelf was set to 500 km.

When surface accumulation is larger than basal melting (or when basal freezing occurs), M is positive, and equation (5.69) can be written as

$$\frac{\partial H}{\partial x} = \frac{MH - CH^{n+2}}{Mx + H_o U_o}. \tag{5.72}$$

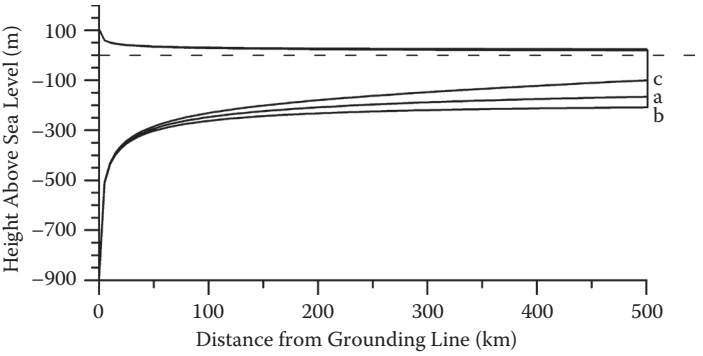

FIGURE 5.11 Equilibrium profile of ice shelves spreading in the along-flow direction only. The thickness at the grounding line equals 1000 m and the speed across the grounding line equals 250 m/yr for all three profiles. The accumulation rate is M = 0 (profile a), M = +0.25 m/yr (profile b), and M = –0.25 m/yr (profile c).

Collecting all terms containing the unknown ice thickness on the left-hand side, this equation is rewritten as

$$\left(\frac{1}{MH} + \frac{\frac{C}{M^2} H^n}{1 - \frac{C}{M} H^{n+1}} \right) \partial H = \frac{1}{Mx + H_o U_o} \partial x. \tag{5.73}$$

Recalling that $\partial(\ln H) = 1/H\, \partial H$, both sides can be integrated to

$$\frac{1}{M} \ln H - \frac{1}{M(n+1)} \ln\left(1 - \frac{C}{M} H^{n+1}\right) = \\ = \frac{1}{M} \ln\left(Mx + H_o U_o\right) + \frac{1}{M(n+1)} \ln D. \tag{5.74}$$

Note how the integration constant (the last term on the right-hand side) is written. Using some elementary rules for manipulating natural logarithms, the following relation is found:

$$H^{n+1} \left(1 - \frac{C}{M} H^{n+1}\right)^{-1} = D\left(Mx + H_o U_o\right)^{n+1}. \tag{5.75}$$

The integration constant, D, follows from the boundary condition that the thickness at the grounding line (at x = 0) must be equal to H_o and

$$D = \frac{1}{U_o^{n+1}\left(1 - \frac{C}{M} H_o^{n+1}\right)}. \tag{5.76}$$

After some more algebraic manipulation, the following expression for the ice thickness is found

$$H = \left(\frac{C}{M} - \frac{U_o^{n+1}\left(\frac{C}{M} H_o^{n+1} - 1 \right)}{(Mx + H_o U_o)^{n+1}} \right)^{-1/(n+1)} . \tag{5.77}$$

Although this expression looks much more complicated than the profile obtained for M = 0 (equation (5.71)), the essential characteristics of the profile are retained, as can be seen in Figure 5.11 (profile b). Near the grounding line, the ice thickness decreases rapidly and then reaches a more or less constant value. For a free-floating ice shelf, the thickness must decrease with distance from the grounding line (otherwise the ice would float back toward the grounding line), or $\partial H/\partial x < 0$. From equation (5.72) it follows that this requires that the ice thickness is greater than a critical value, H_{cr}, given by

$$H_{cr} = \left(\frac{M}{C} \right)^{1/(n+1)} . \tag{5.78}$$

However, as can be seen in Figure 5.11, this critical thickness is reached asymptotically (for the profile shown in Figure 5.11, the critical thickness is 307 m). Therefore, to prevent the shelf from becoming unrealistically large, the maximum length for the profile shown in this figure was set to 500 km, the same length used for profile a (M = 0 m/yr).

The third possibility to be considered is an ice shelf subject to basal and/or surface melting, such that M is negative. Defining $\hat{M} = -M$, equation (5.69) becomes

$$\frac{\partial H}{\partial x} = - \frac{\hat{M} H + C H^{n+2}}{H_o U_o - \hat{M} x} . \tag{5.79}$$

Following a similar procedure as above, the ice-shelf profile is found to be

$$H = \left(\frac{U_o^{n+1}\left(1 + \frac{C}{\hat{M}} H_o^{n+1} \right)}{(H_o U_o - \hat{M} x)^{n+1}} - \frac{C}{\hat{M}} \right)^{-1/(n+1)} . \tag{5.80}$$

Note the similarity between this profile and equation (5.77). Again, the thickness must decrease away from the grounding line. Because all quantities in equation (5.79) are positive, the condition $\partial H/\partial x < 0$ requires that the length of the shelf must be smaller than the critical length, L_{cr}, given by

$$L_{cr} = \frac{H_o U_o}{\hat{M}} . \tag{5.81}$$

For profile c shown in Figure 5.11, this critical length is 533 km. However, to allow for a comparison with the other two profiles, the maximum length was set to 500 km.

The profiles derived above pertain to the very special situation of an ice shelf spreading in one direction, with resistance to flow arising from gradients in longitudinal stress only. This assumption of plane flow is not realistic for a free-floating ice shelf because, if not restricted laterally, the shelf will spread in both horizontal directions. Thus, the plane-flow model applies only to an ice shelf in a parallel-sided bay where lateral drag is negligible. While the two-dimensional profile of an ice shelf spreading in both horizontal directions cannot be easily determined, the effect of lateral spreading on the centerline profile of the shelf can be estimated as discussed below. A more complete treatment of radial ice-shelf flow can be found in Morland (1987) and Morland and Zainuddin (1987).

For uniform spreading in both horizontal directions, the creep rates are given by equation (4.65)

$$\dot{\varepsilon}_{xx} = \dot{\varepsilon}_{yy} = C_2 H^n, \tag{5.82}$$

with

$$C_2 = 3^{-(n+1)/2} \left(\frac{\rho g(\rho_w - \rho)}{2B\rho_w} \right)^n. \tag{5.83}$$

Assuming steady state, the continuity equation is

$$H\frac{\partial U}{\partial x} + U\frac{\partial H}{\partial x} + H\frac{\partial V}{\partial y} + V\frac{\partial H}{\partial y} = M. \tag{5.84}$$

Along the centerline of the shelf, it follows from symmetry arguments that the transverse velocity component, V, is zero and the last term on the left-hand side is zero. Substituting (5.82) for the strain rates gives

$$2C_2 H^{n+1} + U\frac{\partial H}{\partial x} = M. \tag{5.85}$$

Because the flow is two-dimensional, the continuity equation cannot be integrated along the flowline to find an expression for the ice velocity, U (as was done to arrive at equation (5.33) for the case of plane flow). This means that an analytical solution cannot be derived for the centerline profile of an ice shelf spreading in both horizontal directions. However, this profile can be found by numerically integrating the continuity equation (5.85) along the flowline analogous to the method of Sanderson (1979). Rewriting (5.85) as

$$\frac{\partial H}{\partial x} = \frac{1}{U}(M - 2C_2 H^{n+1}), \tag{5.86}$$

the thickness gradient at the grounding line can be estimated from the prescribed thickness, H_o, and velocity, U_o, at the grounding line. This allows the thickness at some distance Δx away from the grounding line to be calculated. From this new thickness, the creep rate $\dot{\varepsilon}_{xx} = \partial U/\partial x$ is calculated using equation (5.82). This allows the

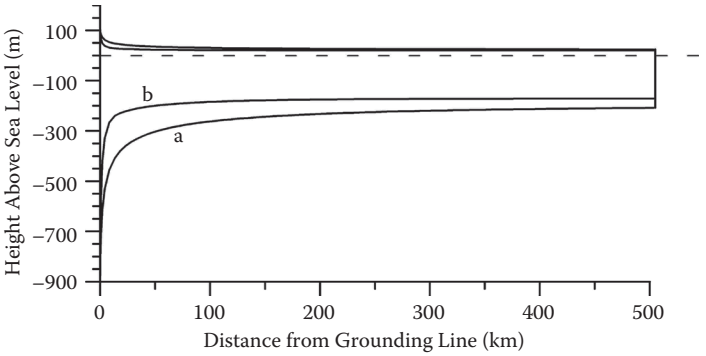

FIGURE 5.12 Equilibrium profile of an ice shelf spreading in the along-flow direction only (profile a) and the profile of an ice shelf spreading in both horizontal directions (profile b). Constants used are H_o = 1000 m, U_o = 250 m/yr, and M = 0.25 m/yr.

velocity to be extrapolated to the new point. With all quantities on the right-hand side of equation (5.86) known, the thickness gradient can be estimated, and the thickness at the next gridpoint determined. This procedure is repeated until some criterion for the maximum length or minimum thickness is reached. Because the thickness decreases very rapidly near the grounding line, the horizontal step, Δx, must be very small (a few meters) in this region to minimize numerical errors. Farther away, the value of Δx may be gradually increased to, say, 5 km. Figure 5.12 shows a centerline profile calculated using this numerical scheme. Also shown is the plane-flow profile given by equation (5.77). Lateral spreading significantly reduces the thickness of the shelf, as a result of mass being lost in the cross-flow direction. The essential characteristics of the profile are similar to those of the plane-flow solutions, however.

5.6 FLOW CONTROLLED BY LATERAL DRAG

The equations for ice-shelf spreading derived in Section 4.5 include the effect of lateral drag, and it was shown that the stretching rate at some point on the shelf depends on the lateral drag integrated over the distance from that point to the ice-shelf terminus. This means that to solve the continuity equation numerically to find the ice-shelf profile, the integration must start at the shelf front (with prescribed thickness and velocity) and proceed upglacier to the grounding line, instead of starting at the grounding line as in the model discussed in the previous section (Sanderson, 1979). An analytical expression for the profile cannot be derived except for the special case of lateral drag supporting all (or most) of the driving stress. This model may apply to a floating ice shelf in a parallel-sided embayment, or to an ice stream decoupled completely from its bed.

If the driving stress is fully supported by drag at the margins, the transverse velocity profile is given by equation (4.51)

$$U(y) = U_c \left(1 - \left(\frac{y}{W}\right)^{n+1}\right), \tag{5.87}$$

where y represents the transverse distance with $y = \pm W$ at the lateral margins (the half-width of the flowband, W, is taken constant here), and U_c the centerline velocity, given by equation (4.52)

$$U_c = \frac{2}{n+1}\left(\frac{\tau_{dx}}{BH}\right)^n W^{n+1}. \tag{5.88}$$

Integrating this expression over the full width of the flowband, the width-averaged discharge velocity is found to be

$$U = \frac{n+1}{n+2} U_c. \tag{5.89}$$

Combining equations (5.89) and (5.88), the width-averaged velocity can be written as

$$U = -A_o \left|\frac{\partial h}{\partial x}\right|^{n-1} \frac{\partial h}{\partial x}, \tag{5.90}$$

with

$$A_o = \frac{2}{n+2} \frac{W^{n+1}}{B^n} (\rho g)^n. \tag{5.91}$$

Substituting expression (5.90) for the width-averaged velocity into the continuity equation (5.68) allows an analytical expression for the profile to be determined for two cases in which the flow is controlled entirely by lateral drag, namely, an ice stream on a flat bed and with constant half-width, and a floating ice shelf in a parallel-sided embayment.

Consider first an ice stream moving over a soft bed unable to offer any significant resistance to flow. As argued by Whillans and Van der Veen (1997), this may be the case for Whillans Ice Stream in West Antarctica, where lateral drag appears to provide all resistance to flow. Taking the bed to be horizontal, the average discharge velocity is

$$U = -A_o \left|\frac{\partial H}{\partial x}\right|^{n-1} \frac{\partial H}{\partial x}. \tag{5.92}$$

As in the previous section, this expression is substituted into the continuity equation (5.68) and integrated in the direction of flow to yield the following profile

$$\left(\frac{H}{H_o}\right)^{1+1/n} = 1 - \frac{U_o^{1+1/n}}{M A_o^{1/n}} \left(\left(\frac{Mx}{H_o U_o} + 1\right)^{1+1/n} - 1\right). \tag{5.93}$$

Here $H_o U_o$ represents the ice flux at the head of the ice stream (at $x = 0$). In the upper panel of Figure 5.13 this ice-stream profile is shown. One prominent feature is the convex curvature of the surface, with the surface slope increasing toward the mouth of the ice stream. This increase in slope is needed to allow the velocity to increase with distance along the flowline, as required for steady state (equation (5.33)).

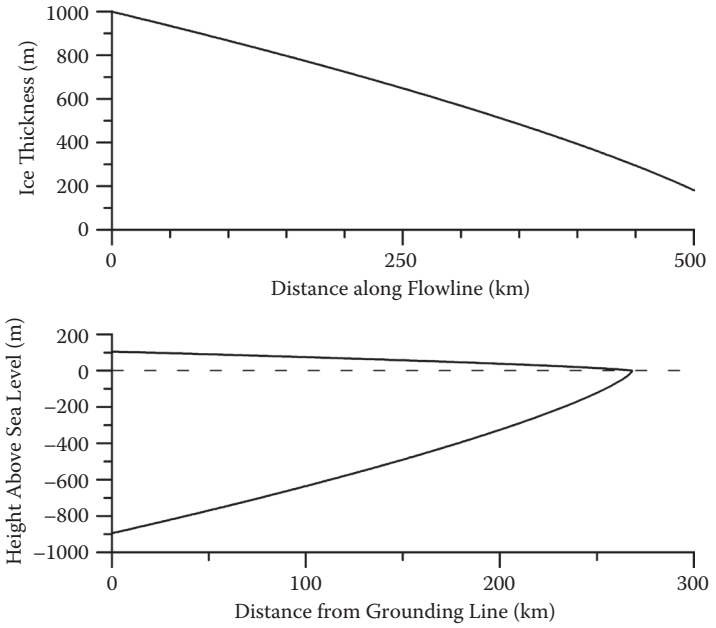

FIGURE 5.13 Equilibrium profile on an ice stream on a horizontal bed (upper panel) and an ice shelf (lower panel), both controlled entirely by lateral drag. Values of constant used are H_o = 1000 m, U_o = 250 m/yr, W = 15 km, and M = 0.15 m/yr.

For an ice shelf, the surface elevation is related to the ice thickness through the flotation criterion

$$h = \left(1 - \frac{\rho}{\rho_w}\right)H, \tag{5.94}$$

and the velocity becomes

$$U = -A_1 \left|\frac{\partial H}{\partial x}\right|^{n-1} \frac{\partial H}{\partial x}. \tag{5.95}$$

The constant, A_1, is related to A_o as

$$A_1 = \left(1 - \frac{\rho}{\rho_w}\right)A_o. \tag{5.96}$$

Thus, the shelf thickness is also given by equation (5.93) but with A_o replaced by A_1. Again, the surface slope increases toward the ice front to maintain mass continuity. Consequently, the resulting profile, shown in Figure 5.13, is essentially different from that of a free-floating ice shelf (Figure 5.11), which is characterized by a concave-upward surface profile.

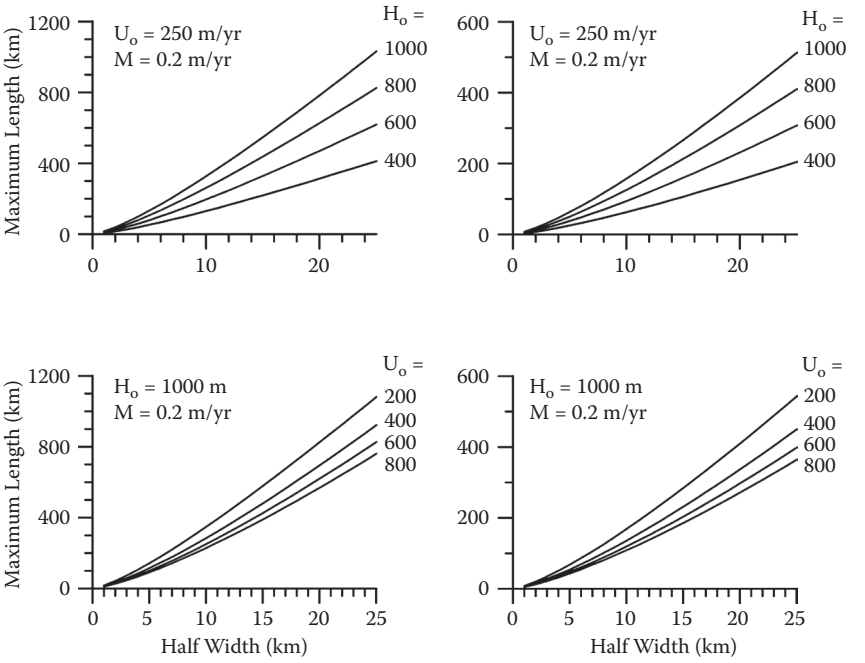

FIGURE 5.14 Maximum length of an ice stream on a horizontal bed (left panels) and of an ice shelf (right panels), both controlled by lateral drag, as a function of the half width, for different values of H_o (in m) (upper panels) and U_o (in m/yr) (lower panels).

The maximum length of the ice stream or ice shelf follows by setting the thickness to zero in equation (5.93). The result is

$$L_{max} = \frac{H_o U_o}{M}\left(\left(\frac{M A_i^{1/n}}{U_o^{1+1/n}} + 1\right)^{n/(1+n)} - 1\right), \tag{5.97}$$

where $A_i = A_o$ for an ice stream on a flat bed, and $A_i = A_l$ for a floating ice shelf. The parameter most critical in determining L_{max} is the half-width, W (Figure 5.14). This is because the ice velocity is proportional to the fourth power of W (if n = 3). Thus, a small increase in width leads to a large increase in speed. To maintain the discharge needed for steady state (which is independent of the width), the thickness gradient (or surface slope) must decrease, allowing the flowband to become longer. Similar arguments can be applied to explain the dependency of L_{max} on the thickness and velocity at the head of the flowband. The accumulation rate, M, has only a minor effect on the maximum length. From equation (5.97) it follows that L_{max} is proportional to $M^{1/4}$, and large changes in accumulation rate are needed to significantly alter the profile along the flowband.